Frontiers of Information Technology & Electronic Engineering
www.jzus.zju.edu.cn; engineering.cae.cn; www.springerlink.com
ISSN 2095-9184 (print); ISSN 2095-9230 (online)
E-mail: jzus@zju.edu.cn

Adaptive output feedback formation tracking for a class of multiagent systems with quantized input signals*

Jing-lin HU†, Xiu-xia SUN, Lei HE, Ri LIU, Xiong-feng DENG

Equipment Management and UAV Engineering College, Air Force Engineering University, Xi'an 710038, China

†E-mail: hujinglineee@163.com

Received Dec. 11, 2016; Revision accepted Mar. 23, 2017; Crosschecked Sept. 9, 2018

Abstract: A novel adaptive output feedback control approach is presented for formation tracking of a multiagent system with uncertainties and quantized input signals. The agents are described by nonlinear dynamics models with unknown parameters and immeasurable states. A high-gain dynamic state observer is established to estimate the immeasurable states. With a proper design parameter choice, an adaptive output feedback control method is developed employing a hysteretic quantizer and the designed dynamic state observer. Stability analysis shows that the control strategy can guarantee that the agents can maintain the formation shape while tracking the reference trajectory. In addition, all the signals in the closed-loop system are bounded. The effectiveness of the control strategy is validated by simulation.

Key words: Multiagent system; Adaptive output feedback; Formation tracking; Hysteretic quantizer
https://doi.org/10.1631/FITEE.1601801 **CLC number:** TP273

1 Introduction

Recently, multiagent system research has raised significant concerns for its huge development potential. It is believed that the multiagent system containing a team of low-cost agents is more effective than a single high-tech system in executing complex missions (Lu et al., 2014; Wan et al., 2016; Zhao et al., 2016b). With a flexible structure, multiagent systems can easily adjust to different tasks such as surveillance, exploration, and firefighting. In addition, multiagent systems are more robust if there is a single agent failure (Mahmood and Kim, 2015; Liu et al., 2016).

Formation control is a significant aspect in multiagent system control problems. Multiagent system control involves the agents forming and maintaining a geometric shape while tracking a desired trajectory (Wen et al., 2015). In formation tracking strategies, the states of agents are commonly controlled through agent dynamics models. A lot of existing works describe the agent dynamics by first- or second-order linear models (Fu and Wang, 2014; Zhao et al., 2017). To improve model precision, many control solutions focus on high-order linear dynamics (Zhao et al., 2016a).

In real applications, complicated nonlinear dynamics always exist in multiagent systems, and are managed in some existing research by establishing nonlinear dynamic models (He WL et al., 2017). A cooperative control design was proposed for multiagent system formation tracking while agents were described by a non-holonomic constrained nonlinear model (Briñón-Arranz et al., 2014). Furthermore, considering that the agents inevitably have a lot of uncertainties in reality, some adaptive control theories have been applied to overcome the uncertainties. While considering that unknown parameters exist in a multiagent system, Liu and Jia (2012) proposed a model reference adaptive control theory to control the formation. Sliding mode theory was introduced for

* Project supported by the National Natural Science Foundation of China (No. 20155896025)
ORCID: Jing-lin HU, http://orcid.org/0000-0003-1566-0848

spacecraft formation control with uncertainty and disturbance parameters (Bae and Kim, 2012). An adaptive backstepping technique was introduced to multiagent system formation control for the unknown parameters and unknown nonlinear dynamics in systems (He L et al., 2017).

Control problems with quantized signals have been intensively investigated in the research of networked control systems (Jiang and Liu, 2013; Wan et al., 2017). The problems of multiagent systems with quantized signals have not received enough notice in typical networked systems, whereas quantized signals widely exist in multiagent systems. Among the agents, the signals need to be quantized before being emitted through network communication channels under a limited bandwidth. However, strong nonlinear characteristics introduced by quantization can cause the system to have a worse control performance or even instability (Li et al., 2017). Quantization can be classified into static or dynamic (Jiang and Liu, 2013). Static quantizers have fixed quantization levels, so static quantization resolution should be increased close to the origin to improve the control performance and decrease quantization errors. During the control process, the dynamic quantizers can adjust the quantization levels to improve the control performance. A hysteretic quantizer was used by Zhou et al. (2014) for its ability to avoid chattering, but the application of the proposed strategy is limited by too many rigorous assumptions (Zhou et al., 2014).

Some important achievements have been made in quantized controllers for linear and nonlinear systems (Liu et al., 2012; Fu and Wang, 2014). Nonlinear systems with a quantized input were investigated by Liu and Elia (2004), who proposed a quantized controller based on the Lyapunov stability theory. However, studies involving adaptive quantized control theories are seldom reported for nonlinear systems with uncertainties. Hayakawa et al. (2009) designed an adaptive control framework to control nonlinear systems with uncertainties and quantized signals, but the framework stability is heavily related to the characteristics of the control signals. Thus, it cannot be used in a real control application. Zhou et al. (2014) used the adaptive control theory and backstepping technique to control a nonlinear system with a strict feedback and quantized input signals. However, too many assumptions limit the choice of the quantization density parameter. Combined with the derivative explosion of the backstepping technique, it will be very difficult to realize the controller for higher-order systems. Note that the current adaptive theories are commonly based on the state feedback, which requires that multiagent systems be equipped with more sensors for state measurement and a larger bandwidth for communication. Compared with that, adaptive output feedback control can lead to a simpler controller design, but the relevant approaches for nonlinear uncertain systems with quantized signals are rarely seen, to the best of our knowledge.

Based on the previous methods and analysis, our research concerns adaptive output feedback formation tracking for a class of multiagent systems with quantized input signals. The agents are described by a nonlinear dynamics model with unknown parameters and immeasurable states. The main contributions are listed as follows:

1. An exact dynamic model is not required. Unknown parameters and immeasurable states in the agents are well solved through an adaptive output feedback control technique and a dynamic high-gain observer.

2. Taking into account quantized input signals, the hysteretic quantizer is introduced to the systems to avoid chattering. In addition, the controller complexity is significantly reduced by the design of less dynamic gains.

3. With the proposed strategy, the multiagent system formation shape is achieved and maintained when agents asymptotically track the reference trajectory. In addition, tracking errors can be limited to an arbitrarily small neighborhood around the origin and all the closed-loop states can be bounded with a proper parameter choice.

2 Problem statement

2.1 Problem description

The networked multiagent systems in this study consist of N fully actuated agents. The agents can be described by a nonlinear system model with unknown parameters and nonidentical, nonlinear dynamics as follows (Rezaee and Abdollahi, 2014):

$$\begin{cases} M_i\ddot{p}_{ix}+B_i\dot{p}_{ix}=q(u_{ix})-k_{i,\mathrm{d}}\dot{p}_{ix}, \\ M_i\ddot{p}_{iy}+B_i\dot{p}_{iy}=q(u_{iy})-k_{i,\mathrm{d}}\dot{p}_{iy}, \end{cases} \tag{1}$$

where $\boldsymbol{p}_i=(p_{ix}, p_{iy})$ is the position of the i^{th} agent, M_i is the agent mass, B_i is the unknown damper parameter, $k_{i,\mathrm{d}}$ is an unknown coefficient considered to control the transient response of the agent, and $(q(u_{ix}), q(u_{iy}))$ is the quantized control input.

Fig. 1 shows the multiagent formation where the three points denote three agents. With a proper design of the quantized controller and the desired formation shape and reference trajectory, the agents can form the formation shape and track the reference trajectory from their appropriate initial positions. In the figure, $(\omega_{ix}, \omega_{iy})$ represents the relative position of the i^{th} agent in the formation, and $(p_{ix,0}, p_{iy,0})$ and (p_{ix}, p_{iy}) represent the initial and final positions of the i^{th} agent, respectively. To avoid leader failure weakness in the leader-follower structure, a virtual structure is used for the formation of the topology structure. In this structure, a virtual leader is used to track the reference trajectory and all the agents can obtain information from the virtual leader. By keeping appropriate relative positions with respect to the virtual leader, all the agents can form the desired formation shape. In this study, the control objective is to design an adaptive controller (u_{ix}, u_{iy}) such that: (1) all the closed-loop signals maintain boundedness; (2) all the agents can follow the reference trajectory $(p_{\mathrm{r}x}, p_{\mathrm{r}y})$ while establishing and maintaining the desired formation shape.

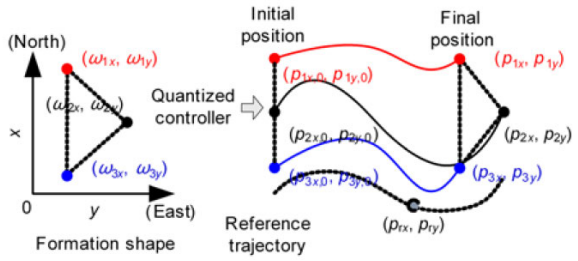

Fig. 1 Multiagent formation illustration

Assumption 1 The reference trajectory signal $(p_{\mathrm{r}x}, p_{\mathrm{r}y})$ and its time derivative are continuous and bounded.

Considering the bounded disturbance that exists in an agent, Eq. (1) can be rewritten as follows when described with state-space techniques:

$$\begin{cases} \dot{x}_{ix,1}=x_{ix,2}+d_{ix,1}, \\ \dot{x}_{ix,2}=q(u_{ix})+\theta_i x_{ix,2}+d_{ix,2}, \\ \overline{p}_{ix}=M_i p_{ix}=x_{ix,1}, \\ \dot{x}_{iy,1}=x_{iy,2}+d_{iy,1}, \\ \dot{x}_{iy,2}=q(u_{iy})+\theta_i x_{iy,2}+d_{iy,2}, \\ \overline{p}_{iy}=M_i p_{iy}=x_{iy,1}, \end{cases} \tag{2}$$

where $\boldsymbol{x}_{ix}=[x_{ix,1}, x_{ix,2}]^{\mathrm{T}}$ and $\boldsymbol{x}_{iy}=[x_{iy,1}, x_{iy,2}]^{\mathrm{T}}$ are system states in the direction of the x- and y-axis, respectively, $\overline{p}_{ix}$ and $\overline{p}_{iy}$ are the system outputs in the direction of the two axes, $\theta_i=(B_i+k_{i,\mathrm{d}})/M_i$ is an unknown parameter, and $\boldsymbol{d}_{ix}=[d_{ix,1}, d_{ix,2}]^{\mathrm{T}}$ and $\boldsymbol{d}_{iy}=[d_{iy,1}, d_{iy,2}]^{\mathrm{T}}$ are bounded disturbances.

Based on the former analysis, it can be concluded that the agent dynamic models in the direction of the two axes are equipped with the form of the following nonlinear systems with uncertainties and quantized inputs:

$$\begin{cases} \dot{x}_1=x_2+\phi_1(\boldsymbol{x},\theta^*(t))+d_1(t), \\ \dot{x}_2=x_3+\phi_2(\boldsymbol{x},\theta^*(t))+d_2(t), \\ \quad\vdots \\ \dot{x}_n=q\big(v(t)\big)+\phi_n(\boldsymbol{x},\theta^*(t))+d_n(t), \\ y=x_1, \end{cases} \tag{3}$$

where $\boldsymbol{x}=[x_1, x_2, \ldots, x_n]^{\mathrm{T}}\in\mathbb{R}^n$ is the system state vector, $y\in\mathbb{R}$ denotes the output, and $\theta^*(t)$: $\mathbb{R}\to\mathbb{R}^m$ is a continuous and bounded time-varying parameter. Without any information, $\phi_i(\boldsymbol{x}, \theta^*(t))$: $\mathbb{R}^n\times\mathbb{R}^m\to\mathbb{R}$ (i=1, 2, …, n) are continuous and locally Lipschitz in the variable state $\boldsymbol{x}$. The bounded disturbances $d_i(t)$ (i=1, 2, …, n) satisfy the inequality $d_i(t)\le\overline{d}$, where $\overline{d}$ is a positive constant. $q(v(t))$ denotes the hysteretic quantizer of the input signals. The controller is designed for the output y to track the reference signal y_{r} and maintain the closed-loop states bounded with any initial condition of state $\boldsymbol{x}(0)$. y_{r} is assumed to be continuous and bounded.

There is an assumption for system (3).

Assumption 2

$$\left|\phi_i(\boldsymbol{x},\theta^*(t))\right|\le\theta\left(1+|y|^p\right)\left(|x_1|+|x_2|+\ldots+|x_i|\right), \tag{4}$$

where positive constant θ is unknown, positive integer p is known, and i=1, 2, …, n.

2.2 Hysteretic quantizer

To reduce chattering, the hysteretic quantizer $q(v(t))$ is defined by Eq. (5) on the bottom of this page, where $u_i=\rho^{1-i}u_{\min}$ (i=1, 2, …, n), $0<\rho<1$, $\delta=(1-\rho)/(1+\rho)$, and $u_{\min}$ represents the dead zone for $q(v(t))$.

In the controller design, the values of some matrices and parameters are decided according to the following lemmas:

Lemma 1 For proper analysis, in Eq. (5), $q(v(t))$ can be regarded as $q(v(t))=v(t)+\zeta_v$, where ζ_v is a nonlinear part and satisfies the following inequality (Zhou et al., 2014):

$$|\zeta_v| \le \delta |v| + u_{\min}. \tag{6}$$

Lemma 2 For any positive number μ, there exist σ_1, $\sigma_2\in\mathbb{R}$, symmetric matrices $\boldsymbol{P}_1$ and $\boldsymbol{P}_2$, and observer gain vector $\boldsymbol{a}=[a_1, a_2, \ldots, a_n]^{\mathrm{T}}$ and controller gain vector $\boldsymbol{k}=[k_1, k_2, \ldots, k_n]^{\mathrm{T}}$, satisfying the following inequalities (Praly and Jiang, 2004; Li et al., 2017):

$$\begin{cases} \sigma_1>0,\ \sigma_2>0,\ \boldsymbol{P}_1>0,\ \boldsymbol{P}_2>0, \\ -\sigma_1\boldsymbol{I}\ge(\boldsymbol{A}-\boldsymbol{a}\boldsymbol{c}^{\mathrm{T}})^{\mathrm{T}}\boldsymbol{P}_1+\boldsymbol{P}_1(\boldsymbol{A}-\boldsymbol{a}\boldsymbol{c}^{\mathrm{T}}), \\ -3\sigma_1\boldsymbol{I}\ge(\boldsymbol{A}-\boldsymbol{b}\boldsymbol{k}^{\mathrm{T}})^{\mathrm{T}}\boldsymbol{P}_2+\boldsymbol{P}_2(\boldsymbol{A}-\boldsymbol{b}\boldsymbol{k}^{\mathrm{T}}), \\ \mu\boldsymbol{P}_1\le\boldsymbol{D}\boldsymbol{P}_1+\boldsymbol{P}_1\boldsymbol{D}+2\mu\boldsymbol{P}_1\le\sigma_2\boldsymbol{P}_1, \\ \mu\boldsymbol{P}_2\le\boldsymbol{D}\boldsymbol{P}_2+\boldsymbol{P}_2\boldsymbol{D}+2\mu\boldsymbol{P}_2\le\sigma_2\boldsymbol{P}_2, \end{cases} \tag{7}$$

where matrices $\boldsymbol{A}$, $\boldsymbol{D}\in\mathbb{R}^{n\times n}$ and vectors $\boldsymbol{b}$, $\boldsymbol{c}\in\mathbb{R}^n$ are defined as

$$\boldsymbol{A}=\begin{bmatrix}\boldsymbol{0} & \boldsymbol{I}_{n-1}\\ \boldsymbol{0} & \boldsymbol{0}\end{bmatrix},$$
$$\boldsymbol{b}=\begin{bmatrix}0\\0\\\vdots\\0\\1\end{bmatrix},\ \boldsymbol{c}=\begin{bmatrix}1\\0\\0\\\vdots\\0\end{bmatrix},\ \boldsymbol{D}=\begin{bmatrix}0 & & & \\ & 1 & & \\ & & \ddots & \\ & & & n-1\end{bmatrix}. \tag{8}$$

Remark 1 The constant $\rho\in(0, 1)$, which is called the density constant, is the quantization measurement. When the value of ρ is set smaller, the quantizer is coarser. In consideration of $\delta=(1-\rho)/(1+\rho)$, it is clear that the quantizer has fewer quantization degrees when δ is chosen close to 1.

Remark 2 The positive constant μ should be determined to satisfy the inequality $0<2\mu p<1$. Then the parameter set $\{\sigma_1, \sigma_2, \boldsymbol{P}_1, \boldsymbol{P}_2, \boldsymbol{a}, \boldsymbol{k}\}$ is chosen to guarantee inequality (7).

3 Controller design and stability analysis

With uncertainties and hysteretic input quantizer (5), the nonlinear system (3) is controlled by an adaptive output feedback control strategy. Then the closed-loop system stability is analyzed.

3.1 Control strategy design

The designed control strategy contains a high-gain controller and a correlative dynamic observer:

$$\begin{cases} \dot{\hat{x}}_1=\hat{x}_2+la_1(y-y_{\mathrm{r}}-\hat{x}_1), \\ \dot{\hat{x}}_2=\hat{x}_3+l^2a_2(y-y_{\mathrm{r}}-\hat{x}_1), \\ \quad\vdots \\ \dot{\hat{x}}_n=q(v(t))+l^na_n(y-y_{\mathrm{r}}-\hat{x}_1), \\ v=-l^nk_1\hat{x}_1-l^{n-1}k_1\hat{x}_1-\ldots-lk_n\hat{x}_n, \end{cases} \tag{9}$$

$$q(v(t))=\begin{cases} u_i\,\mathrm{sgn}(v), & \dfrac{u_i}{1+\delta}<|v|\le u_i,\dot{v}<0,\ \text{or}\ u_i<|v|\le\dfrac{u_i}{1-\delta},\dot{v}>0, \\ u_i(1+\delta)\,\mathrm{sgn}(v), & u_i<|v|\le\dfrac{u_i}{1-\delta},\dot{v}<0,\ \text{or}\ \dfrac{u_i}{1-\delta}<|v|\le\dfrac{u_i(1+\delta)}{1-\delta},\dot{v}>0, \\ 0, & 0<|v|\le\dfrac{u_{\min}}{1+\delta},\dot{v}<0,\ \text{or}\ \dfrac{u_{\min}}{1+\delta}<|v|\le u_{\min},\dot{v}>0, \\ q(v(t^-)), & \dot{v}=0. \end{cases} \tag{5}$$

where $\hat{\boldsymbol{x}}=[\hat{x}_1,\hat{x}_2,\ldots,\hat{x}_n]^{\mathrm{T}}\in\mathbb{R}^n$ is the state vector of the observer. Gain vectors $\boldsymbol{a}$ and $\boldsymbol{k}$ are determined based on Lemma 2. The dynamic gain l is updated by

$$\begin{aligned}\dot{l}&=g(l,y,\hat{x}_1,y_{\mathrm{r}})\\&=\max\left\{-\alpha_1 l^2+\alpha_2 l\left(1+|y|^p\right)^2,\right.\\&\qquad\left.(y-y_{\mathrm{r}}-\hat{x}_1)^2+\hat{x}_1^2-\varsigma,\ 0\right\},\end{aligned}\tag{10}$$

where parameters ς, α_1, and α_2 are designed as positive constants. The initial condition of l is $l(0)=1$. Note that in region $(l,y,\hat{x}_1)$, $g(l,y,\hat{x}_1,y_{\mathrm{r}})$ is locally Lipschitz. In addition, $g(l,y,\hat{x}_1,y_{\mathrm{r}})$ is a continuous function in y_{r}. Therefore, dynamic gain l has the following characteristics:

$$\begin{cases}l\ge 1,\\ \dot{l}\ge-\alpha_1 l^2+\alpha_2 l\left(1+|y|^p\right)^2,\dot{l}\ge 0,\\ \dot{l}\ge(y-y_{\mathrm{r}}-\hat{x}_1)^2+\hat{x}_1^2-\varsigma.\end{cases}\tag{11}$$

Remark 3 The update law of l is proposed for the adaptive controller to adjust to the system nonlinearity, parameter uncertainty, and disturbance influence. In addition, the design parameter ς is introduced to realize the system's adaptive tracking. Our controller design needs only one dynamic gain, which greatly reduces the controller complexity.

With a hysteretic quantizer introduced in the system, the main theory in this study can be summed up as follows:

Theorem 1 Under the condition that Assumptions 1 and 2 hold and the parameter μ in Lemma 2 is set to satisfy $0<2\mu p<1$, a closed-loop system is considered that consists of plant (3), hysteretic quantizer (5), output feedback controller (9), and update law (10). If the quantizer coefficient δ satisfies

$$2\delta\|\boldsymbol{P}_2\boldsymbol{b}\|\|\boldsymbol{k}\|\le\sigma_1,\tag{12}$$

then all the states in the closed-loop system remain bounded, and the tracking error $y-y_{\mathrm{r}}$ can be steered to within a small neighborhood of the origin.

According to the controller design of Eqs. (7)–(10), for the i^{th} agent in multiagent formation, the high-gain observer, high-gain controller, and update law of dynamic gain are designed as follows:

1. In the x-axis direction, we have

$$\begin{cases}\dot{\hat{x}}_{ix,1}=\dot{\hat{x}}_{ix,2}+l_{ix}a_{i1}\left[\bar{p}_{ix}-(\bar{p}_{\mathrm{r}x}+\bar{\omega}_{ix})-\hat{x}_{ix,1}\right],\\ \dot{\hat{x}}_{ix,2}=q(u_{ix})+l_{ix}^2a_{i2}\left[\bar{p}_{ix}-(\bar{p}_{\mathrm{r}x}+\bar{\omega}_{ix})-\hat{x}_{ix,1}\right],\\ u_{ix}=-l_{ix}^2k_{i1}\hat{x}_{ix,1}-l_{ix}k_{i2}\hat{x}_{ix,2},\\ \dot{l}_{ix}=\max\left\{0,\ -\alpha_{i1}l_{ix}^2+\alpha_{i2}l_{ix}\left(1+|\bar{p}_{ix}|^p\right)^2,\right.\\ \qquad\left.\left[\bar{p}_{ix}-(\bar{p}_{\mathrm{r}x}+\bar{\omega}_{ix})-\hat{x}_{ix,1}\right]^2+\hat{x}_{ix,1}^2-\varsigma_i\right\}.\end{cases}\tag{13}$$

In Eq. (13), $\hat{\boldsymbol{x}}_{ix}=\left[\hat{x}_{ix,1},\hat{x}_{ix,2}\right]^{\mathrm{T}}$ is the observer state, $\bar{p}_{\mathrm{r}x}=M_i p_{\mathrm{r}x}$, $\bar{\omega}_{ix}=M_i\omega_{ix}$, and $l_{ix}(0)=1$.

2. In the y-axis direction, we have

$$\begin{cases}\dot{\hat{x}}_{iy,1}=\dot{\hat{x}}_{iy,2}+l_{iy}a_{i1}\left[\bar{p}_{iy}-(\bar{p}_{\mathrm{r}y}+\bar{\omega}_{iy})-\hat{x}_{iy,1}\right],\\ \dot{\hat{x}}_{iy,2}=q(u_{iy})+l_{iy}^2a_{i2}\left[\bar{p}_{iy}-(\bar{p}_{\mathrm{r}y}+\bar{\omega}_{iy})-\hat{x}_{iy,1}\right],\\ u_{iy}=-l_{iy}^2k_{i1}\hat{x}_{iy,1}-l_{iy}k_{i2}\hat{x}_{iy,2},\\ \dot{l}_{iy}=\max\left\{0,\ -\alpha_{i1}l_{iy}^2+\alpha_{i2}l_{iy}\left(1+|\bar{p}_{iy}|^p\right)^2,\right.\\ \qquad\left.\left[\bar{p}_{iy}-(\bar{p}_{\mathrm{r}y}+\bar{\omega}_{iy})-\hat{x}_{iy,1}\right]^2+\hat{x}_{iy,1}^2-\varsigma_i\right\}.\end{cases}\tag{14}$$

In Eq. (14), $\hat{\boldsymbol{x}}_{iy}=\left[\hat{x}_{iy,1},\hat{x}_{iy,2}\right]^{\mathrm{T}}$ is the observer state, $\bar{p}_{\mathrm{r}y}=M_i p_{\mathrm{r}y}$, $\bar{\omega}_{iy}=M_i\omega_{iy}$, and $l_{iy}(0)=1$.

3.2 Stability analysis

Define the estimation errors of system (3) as

$$\begin{cases}\boldsymbol{e}=\boldsymbol{x}-\boldsymbol{Y}_{\mathrm{r}}-\hat{\boldsymbol{x}},\\ \boldsymbol{Y}_{\mathrm{r}}=[y_{\mathrm{r}},0,0,\ldots,0]^{\mathrm{T}}.\end{cases}\tag{15}$$

Based on Eqs. (3) and (9), the estimation error dynamics can be established as

$$\begin{cases}\dot{e}_1=e_2-la_1e_1+\phi_1(\boldsymbol{x},\theta^*(t))+d_1(t)-\dot{y}_{\mathrm{r}},\\ \dot{e}_2=e_3-l^2a_2e_1+\phi_2(\boldsymbol{x},\theta^*(t))+d_2(t),\\ \quad\vdots\\ \dot{e}_n=-l^na_ne_1+\phi_n(\boldsymbol{x},\theta^*(t))+d_n(t).\end{cases}\tag{16}$$

With the help of the following transformations:

$$\bar{e}_i=\frac{e_i}{l^{i-1+\mu}},\ \ \bar{x}_i=\frac{\hat{x}_i}{l^{i-1+\mu}},\ i=1,2,\ldots,n, \tag{17}$$

Eqs. (9) and (16) can be rewritten as

$$\begin{cases}\dot{\bar{\boldsymbol{x}}}=l(\boldsymbol{A}-\boldsymbol{b}\boldsymbol{k}^{\mathrm{T}})\bar{\boldsymbol{x}}+l\boldsymbol{a}\bar{e}_1-\dfrac{\dot{l}}{l}(\mu\boldsymbol{I}+\boldsymbol{D})\bar{\boldsymbol{x}},\\ \dot{\bar{\boldsymbol{e}}}=l(\boldsymbol{A}-\boldsymbol{a}\boldsymbol{c}^{\mathrm{T}})\bar{\boldsymbol{e}}+\boldsymbol{L}^{-1}(\boldsymbol{\Phi}+\boldsymbol{d}-\dot{\boldsymbol{Y}}_{\mathrm{r}})\dfrac{\dot{l}}{l}(\mu\boldsymbol{I}+\boldsymbol{D})\bar{\boldsymbol{e}},\end{cases} \tag{18}$$

where $\boldsymbol{\Phi}=[\phi_1,\ \phi_2,\ \ldots,\ \phi_n]^{\mathrm{T}}$, $\boldsymbol{d}=[d_1,\ d_2,\ \ldots,\ d_n]^{\mathrm{T}}$, and $\boldsymbol{L}=l^{\mu}\mathrm{diag}\{1,\ l,\ l^2,\ \ldots,\ l^{n-1}\}$.

Under Lemma 2, when μ is chosen to satisfy $0<2\mu p<1$, $\{\sigma_1,\ \sigma_2,\ \boldsymbol{P}_1,\ \boldsymbol{P}_2,\ \boldsymbol{a},\ \boldsymbol{k}\}$ can be calculated to satisfy inequality (7). With the matrices $\boldsymbol{P}_1$ and $\boldsymbol{P}_2$ designed, the Lyapunov function is constructed as follows:

$$V=\eta\bar{\boldsymbol{e}}^{\mathrm{T}}\boldsymbol{P}_1\bar{\boldsymbol{e}}+\bar{\boldsymbol{x}}^{\mathrm{T}}\boldsymbol{P}_2\bar{\boldsymbol{x}}, \tag{19}$$

where $\eta=\|\boldsymbol{P}_2\boldsymbol{a}\|^2/\sigma_1^2+1$. The time derivative of V along the trajectory of system (18) can result in

$$\begin{aligned}\dot{V}\le&-\eta\sigma_1 l\|\bar{\boldsymbol{e}}\|^2+2\eta\bar{\boldsymbol{e}}^{\mathrm{T}}\boldsymbol{P}_1\boldsymbol{L}^{-1}(\boldsymbol{\Phi}+\boldsymbol{d}-\dot{\boldsymbol{Y}}_{\mathrm{r}})\\&-\eta\frac{\dot{l}}{l}\bar{\boldsymbol{e}}^{\mathrm{T}}(\boldsymbol{D}\boldsymbol{P}_1+\boldsymbol{P}_1\boldsymbol{D}+2\mu\boldsymbol{P}_1)\bar{\boldsymbol{e}}-3\sigma_1 l\|\bar{\boldsymbol{x}}\|^2\\&+2l\bar{\boldsymbol{x}}^{\mathrm{T}}\boldsymbol{P}_2\boldsymbol{a}\bar{e}_1+2\bar{\boldsymbol{x}}^2\boldsymbol{P}_2\boldsymbol{b}\frac{q(v)-v}{l^{n-1+\mu}}\\&-\frac{\dot{l}}{l}\bar{\boldsymbol{x}}^{\mathrm{T}}(\boldsymbol{D}\boldsymbol{P}_2+\boldsymbol{P}_2\boldsymbol{D}+2\mu\boldsymbol{P}_2)\bar{\boldsymbol{x}}.\end{aligned} \tag{20}$$

From inequality (11), it is clear that $l\ge1$ for $t\in[0,\ t_{\mathrm{f}})$. Thus, with the notation of η, the following inequalities hold:

$$\begin{aligned}2l\bar{\boldsymbol{x}}^{\mathrm{T}}\boldsymbol{P}_2\boldsymbol{a}\bar{e}_1&\le\sigma_1 l\|\bar{\boldsymbol{x}}\|^2+\frac{\|\boldsymbol{P}_2\boldsymbol{a}\|^2}{\sigma_1}l\|\bar{\boldsymbol{e}}\|^2\\&\le\sigma_1 l\|\bar{\boldsymbol{x}}\|^2+(\eta-1)\sigma_1 l\|\bar{\boldsymbol{e}}\|^2,\end{aligned} \tag{21}$$

$$\frac{\dot{l}}{l}\ge-\alpha_1 l+\alpha_2\left(1+|y|^p\right)^2. \tag{22}$$

Therefore, with the conclusion from Lemma 2, inequality (20) can be further expressed as

$$\begin{aligned}\dot{V}\le&-\sigma_1 l\|\bar{\boldsymbol{e}}\|^2-\eta\alpha_2\mu\lambda_1\left(1+|y|^p\right)^2\|\bar{\boldsymbol{e}}\|^2\\&+\alpha_1\sigma_2\|\boldsymbol{P}_1\|l\|\bar{\boldsymbol{x}}\|^2-\alpha_2\mu\lambda_2\left(1+|y|^p\right)^2\|\bar{\boldsymbol{x}}\|^2\\&+2\eta\|\bar{\boldsymbol{e}}\|\|\boldsymbol{P}_1\|\|\boldsymbol{L}^{-1}(\boldsymbol{\Phi}+\boldsymbol{d}-\dot{\boldsymbol{Y}}_{\mathrm{r}})\|+\eta\alpha_1\sigma_2\|\boldsymbol{P}_1\|l\|\bar{\boldsymbol{e}}\|^2\\&-2\sigma_1 l\|\bar{\boldsymbol{x}}\|^2+2\bar{\boldsymbol{x}}^2\boldsymbol{P}_2\boldsymbol{b}\frac{q(v)-v}{l^{n-1+\mu}},\end{aligned} \tag{23}$$

where λ_1 and λ_2 are the minimum eigenvalues of matrices $\boldsymbol{P}_1$ and $\boldsymbol{P}_2$, respectively.

Using Assumption 2, inequality (11), and $d_i(t)\le\bar{d}$, we have

$$\begin{aligned}&\|\boldsymbol{L}^{-1}(\boldsymbol{\Phi}+\boldsymbol{d}-\dot{\boldsymbol{Y}}_{\mathrm{r}})\|\\&\le\frac{1}{l^{\mu}}|\dot{y}_{\mathrm{r}}|+\sum_{i=1}^{n}\frac{1}{l^{i-1+\mu}}\left[\theta\left(1+|y|^p\right)\sum_{j=1}^{i}|x_j|+\bar{d}\right]\\&\le\frac{1}{l^{\mu}}\left[n\bar{d}+|\dot{y}_{\mathrm{r}}|+n\theta\left(1+|y|^p\right)|y_{\mathrm{r}}|\right]\\&\quad+\sum_{i=1}^{n}\sum_{j=1}^{i}\theta\left(1+|y|^p\right)\left(|\bar{e}_j|+|\bar{x}_j|\right)\\&\le n^2\theta\left(1+|y|^p\right)\left(|\bar{e}_j|+|\bar{x}_j|\right)\\&\quad+\frac{1}{l^{\mu}}\left[n\bar{d}+|\dot{y}_{\mathrm{r}}|+n\theta\left(1+|y|^p\right)|y_{\mathrm{r}}|\right].\end{aligned} \tag{24}$$

Thus, with the completion of the square, we obtain

$$\begin{aligned}&2\eta\|\bar{\boldsymbol{e}}\|\|\boldsymbol{P}_1\|\|\boldsymbol{L}^{-1}(\boldsymbol{\Phi}+\boldsymbol{d}-\dot{\boldsymbol{Y}}_{\mathrm{r}})\|\\&\le2\eta^2n^4\|\boldsymbol{P}_1\|^2\theta^2\|\bar{\boldsymbol{e}}\|^2+2\left(1+|y|^p\right)^2\|\bar{\boldsymbol{e}}\|^2\\&\quad+\left(1+|y|^p\right)^2\|\bar{\boldsymbol{x}}\|^2+\frac{1}{4}\sigma_1 l\|\bar{\boldsymbol{e}}\|^2+\frac{1}{l^{2\mu}}\tilde{d},\end{aligned} \tag{25}$$

where $\tilde{d}=\eta^2n^2\|\boldsymbol{P}_1\|^2\theta^2y_{\mathrm{r}}^2+4\eta^2\|\boldsymbol{P}_1\|^2(n\bar{d}+\dot{y}_{\mathrm{r}})^2/\sigma_1$ is bounded. Substituting inequality (25) into inequality (23) results in

$$\begin{aligned}\dot{V}\le&-\left(\frac{3}{4}\sigma_1-\eta\alpha_1\sigma_2\|\boldsymbol{P}_1\|\right)l\|\bar{\boldsymbol{e}}\|^2+2\eta^2n^4\|\boldsymbol{P}_1\|^2\theta^2\|\bar{\boldsymbol{e}}\|^2\\&+2\bar{\boldsymbol{x}}^2\boldsymbol{P}_2\boldsymbol{b}\frac{q(v)-v}{l^{n-1+\mu}}-(\eta\alpha_2\mu\lambda_1-2)\left(1+|y|^p\right)^2\|\bar{\boldsymbol{e}}\|^2\\&-(2\sigma_1-\alpha_1\sigma_2\|\boldsymbol{P}_2\|)l\|\bar{\boldsymbol{x}}\|^2\\&-(\alpha_2\mu\lambda_2-1)\left(1+|y|^p\right)^2\|\bar{\boldsymbol{x}}\|^2+\frac{1}{l^{2\mu}}\tilde{d}.\end{aligned} \tag{26}$$

Taking the hysteretic quantizer (5) into consideration, the following inequality holds by Lemma 1:

$$\frac{q(v)-v}{l^{n-1+\mu}} \le \delta l \left| \frac{v}{l^{n+\mu}} \right| + \frac{u_{\min}}{l^{n-1+\mu}} \le \delta l \left| \boldsymbol{k}^{\mathrm{T}} \bar{\boldsymbol{x}} \right| + \frac{u_{\min}}{l^{n-1+\mu}}. \quad (27)$$

With the quantization parameter design condition (12), the following inequality can be obtained:

$$\begin{aligned} & 2\bar{\boldsymbol{x}}^{\mathrm{T}} \boldsymbol{P}_2 \boldsymbol{b} \frac{q(v)-v}{l^{n-1+\mu}} \\ & \le 2\delta \left\| \boldsymbol{P}_2 \boldsymbol{b} \right\| \left\| \boldsymbol{k} \right\| l \left\| \bar{\boldsymbol{x}} \right\|^2 + \left\| \boldsymbol{P}_2 \boldsymbol{b} \right\|^2 \left\| \bar{\boldsymbol{x}} \right\|^2 + \frac{u_{\min}^2}{l^{2(n-1+\mu)}} \\ & \le \sigma_1 l \left\| \bar{\boldsymbol{x}} \right\|^2 + \left\| \boldsymbol{P}_2 \boldsymbol{b} \right\|^2 \left\| \bar{\boldsymbol{x}} \right\|^2 + \frac{u_{\min}^2}{l^{2(n-1+\mu)}}. \end{aligned} \quad (28)$$

Substituting inequality (28) into inequality (26) yields

$$\begin{aligned} \dot{V} \le & -\left(\frac{3}{4}\sigma_1 - \eta\alpha_1\sigma_2 \left\| \boldsymbol{P}_1 \right\| \right) l \left\| \bar{\boldsymbol{e}} \right\|^2 + \frac{u_{\min}^2}{l^{2(n-1+\mu)}} + \frac{1}{l^{2\mu}} \tilde{d} \\ & - \left(\eta\alpha_2\mu\lambda_1 - 2 \right) \left(1 + |y|^p \right)^2 \left\| \bar{\boldsymbol{e}} \right\|^2 \\ & - \left(\alpha_2\mu\lambda_2 - 1 - \left\| \boldsymbol{P}_2 \boldsymbol{b} \right\|^2 \right) \left(1 + |y|^p \right)^2 \left\| \bar{\boldsymbol{x}} \right\|^2 \\ & + 2\eta^2 n^4 \left\| \boldsymbol{P}_1 \right\|^2 \theta^2 \left\| \bar{\boldsymbol{e}} \right\|^2 - \left(\sigma_1 - \alpha_1\sigma_2 \left\| \boldsymbol{P}_2 \right\| \right) l \left\| \bar{\boldsymbol{x}} \right\|^2. \end{aligned} \quad (29)$$

Design α_1 and α_2 as follows:

$$\begin{cases} \alpha_1 \le \min\left\{ \dfrac{\sigma_1}{2\sigma_2 \left\| \boldsymbol{P}_2 \right\|}, \dfrac{\sigma_1}{2\eta\sigma_2 \left\| \boldsymbol{P}_1 \right\|} \right\}, \\ \alpha_2 \ge \max\left\{ \dfrac{2}{\eta\mu\lambda_1}, \dfrac{1 + \left\| \boldsymbol{P}_2 \boldsymbol{b} \right\|^2}{\mu\lambda_2} \right\}. \end{cases} \quad (30)$$

Now it can be summarized as

$$\begin{aligned} \dot{V} \le & -\frac{1}{4}\sigma_1 l \left\| \bar{\boldsymbol{e}} \right\|^2 - \frac{1}{2}\sigma_1 l \left\| \bar{\boldsymbol{x}} \right\|^2 + \frac{u_{\min}^2}{l^{2(n-1+\mu)}} + \frac{1}{l^{2\mu}} \tilde{d} \\ & + 2\eta^2 n^4 \left\| \boldsymbol{P}_1 \right\|^2 \theta^2 \left\| \bar{\boldsymbol{e}} \right\|^2. \end{aligned} \quad (31)$$

To prove the boundedness of closed-loop system states when $t \in [0, t_f)$, we propose that $l(t)$ and states $\bar{\boldsymbol{x}}(t)$ and $\bar{\boldsymbol{e}}(t)$ remain bounded with $t \in [0, t_f)$. It will be proved in the next section.

Based on this proposition and Eq. (15), the closed-loop system states $(\boldsymbol{x}, \hat{\boldsymbol{x}}, l)$ remain bounded on $[0, t_f)$ and $t_f = +\infty$. Thus, $\boldsymbol{x}(t)$, $\hat{\boldsymbol{x}}(t)$, and $l(t)$ are bounded with $t \in [0, +\infty)$.

In what follows, we show that the tracking error can be steered to be within a small neighborhood of the origin asymptotically. Because $l(t)$ is bounded by $t \in [0, +\infty)$, we see that $\int_0^{+\infty} \dot{l}(t)\mathrm{d}t < +\infty$. Note that $g(l, y, \hat{x}_1, y_r)$ is locally Lipschitz in its independent variables. With the boundedness of $(l, y, \hat{x}_1, y_r)$, there exists a positive constant C that makes the following formula hold for any $t_1, t_2 \in [0, +\infty)$:

$$\begin{aligned} \left| \dot{l}(t_1) - \dot{l}(t_2) \right| &= \left| g(t_1) - g(t_2) \right| \\ &\le C \Big[\left| l(t_1) - l(t_2) \right| + \left| y(t_1) - y(t_2) \right| \\ &\quad + \left| \hat{x}_1(t_1) - \hat{x}_1(t_2) \right| + \left| y_r(t_1) - y_r(t_2) \right| \Big]. \end{aligned} \quad (32)$$

For any positive constant ε, there always exists a $\delta(\varepsilon) > 0$ that makes the following inequality hold:

$$\begin{aligned} & \left| l(t_1) - l(t_2) \right| + \left| y(t_1) - y(t_2) \right| \\ & \quad + \left| \hat{x}_1(t_1) - \hat{x}_1(t_2) \right| + \left| y_r(t_1) - y_r(t_2) \right| < \frac{\varepsilon}{C}, \end{aligned} \quad (33)$$

where t_1 and t_2 satisfy $|t_1 - t_2| \le \delta(\varepsilon)$.

Based on the former condition and inequalities (32) and (33), we can obtain $\left| \dot{l}(t_1) - \dot{l}(t_2) \right| \le \varepsilon$ with $|t_1 - t_2| \le \delta(\varepsilon)$. It is concluded that $\dot{l}(t)$ is uniformly continuous on $[0, +\infty)$.

Barbalat's lemma suggests $\lim_{x \to +\infty} \dot{l}(t) = 0$. With $y - y_r = (y - y_r + \hat{x}_1) - \hat{x}_1$ and inequality (11), we have

$$0 \le (y - y_r + \hat{x}_1)^2 + \hat{x}_1^2 \le \dot{l} + \varsigma. \quad (34)$$

Thus, $0 \le (y - y_r)^2 \le 2(\dot{l} + \varsigma)$. In conclusion, the tracking error $(y - y_r)$ can be steered to within a small neighborhood of the origin by choosing a sufficiently small ς.

4 Proposition proof

4.1 Boundedness proof of $l(t)$

Because $\dot{l} \geq 0$ with $t \in [0, t_f)$, $l(t)$ is monotonically nondecreasing in the same time interval. Suppose $\lim_{x\to+\infty} l(t) = +\infty$, and a finite time $t_1 \in [0, t_f)$ exists satisfying $l(t) \geq 16\eta^2 n^4 \|\boldsymbol{P}_1\|^2 \theta^2 / \sigma_1$ on $[t_1, t_f)$. Considering inequality (31), we have

$$\dot{V} \leq -\frac{1}{8}\sigma_1 l \|\bar{\boldsymbol{e}}\|^2 - \frac{1}{2}\sigma_1 l \|\bar{\boldsymbol{x}}\|^2 + \frac{u_{\min}^2}{l^{2\mu}} + \frac{1}{l^{2\mu}}\tilde{d}, \forall t \in [t_1, t_f). \tag{35}$$

Thus, $\|\bar{\boldsymbol{e}}\|$ and $\|\bar{\boldsymbol{x}}\|$ remain bounded when $t_1 \in [t_1, t_f)$. With $0<2\mu p<1$, we have

$$\begin{aligned} &-\alpha_1 l^2 + \alpha_2 l\left(1+|y|^p\right)^2 \\ &= -\alpha_1 l^2 + \alpha_2 l\left(1+\left|e_1 + y_r + \hat{x}_1\right|^p\right)^2 \\ &= -\alpha_1 l^2 + \alpha_2 l\left(1+l^{\mu p}\left|\bar{e}_1 + l^{-\mu p} y_r + \bar{x}_1\right|^p\right)^2 \\ &\leq -\alpha_1 l^2 + \alpha_2 l^{1+2\mu p}\left(1+l^{\mu p}\left|\bar{e}_1 + l^{-\mu p} y_r + \bar{x}_1\right|^p\right)^2. \end{aligned} \tag{36}$$

Therefore, a finite time t_2 ($t_1<t_2<t_f$) exists, in which inequality $-\alpha_1 l^2 + \alpha_2 l\left(1+|y|^p\right)^2 < 0$ holds in $t \in [t_2, t_f)$, and the following inequality holds:

$$\begin{aligned} \dot{l} &= \max\left\{e_1^2 + \hat{x}_1^2 - \varsigma, 0\right\} \\ &\leq l^{2\mu}\bar{e}_1^2 + l^{2\mu}\bar{x}_1^2 \leq l\bar{e}_1^2 + l\bar{x}_1^2, \ \forall t \in [t_2, t_f). \end{aligned} \tag{37}$$

Then two cases of t_f are considered as follows:

1. $t_f<+\infty$

By integrating the two sides of inequality (35), we have

$$\begin{aligned} &V(t) + \int_{T_2}^{t} \frac{1}{8}\sigma_1 l(\tau)\|\bar{\boldsymbol{e}}(\tau)\|^2 \,\mathrm{d}\tau + \int_{T_2}^{t} \frac{1}{2}\sigma_1 l(\tau)\|\bar{\boldsymbol{x}}(\tau)\|^2 \,\mathrm{d}\tau \\ &\leq V(T_2) + (t-T_2)(u_{\min}^2 + \tilde{d}) < +\infty, \ \forall t \in [t_2, t_f). \end{aligned} \tag{38}$$

Based on inequality (38) and $\dot{l} \leq l\bar{e}_1^2 + l\bar{x}_1^2$ on $[t_2, t_f)$, we have

$$\begin{aligned} l(t) &= l(T_2) + \int_{T_2}^{t} \dot{l}(\tau)\mathrm{d}\tau \\ &\leq l(T_2) + \int_{T_2}^{t} l(\tau)\bar{e}_1^2(\tau)\mathrm{d}\tau + \int_{T_2}^{t} l(\tau)\bar{x}_1^2(\tau)\mathrm{d}\tau \\ &\leq l(T_2) + \int_{T_2}^{t} l(\tau)\|\bar{\boldsymbol{e}}(\tau)\|^2 \,\mathrm{d}\tau + \int_{T_2}^{t} l(\tau)\|\bar{\boldsymbol{x}}(\tau)\|^2 \,\mathrm{d}\tau \\ &\leq l(T_2) + \frac{10}{\sigma_1}\left[V(T_2) + (t-T_2)(u_{\min}^2 + \tilde{d})\right] \\ &\leq +\infty, \quad \forall t \in [t_2, t_f). \end{aligned} \tag{39}$$

This contradicts the assumption $\lim_{x\to+\infty} l(t) = +\infty$.

2. $t_f=+\infty$

Let $V_1=l^{2\mu}V$. With Eq. (10) and inequalities (35) and (37), the derivative of V_1 can yield

$$\begin{aligned} \dot{V}_1 &\leq -\frac{1}{8}\sigma_1 l^{1+2\mu}\|\bar{\boldsymbol{e}}\|^2 - \frac{1}{2}\sigma_1 l^{1+2\mu}\|\bar{\boldsymbol{x}}\|^2 + (u_{\min}^2 + \tilde{d}) \\ &\quad + (\bar{e}_1^2 + \bar{x}_1^2) l^{2\mu} V \\ &\leq -2C_1 l V_1 + (\bar{e}_1^2 + \bar{x}_1^2) V_1 + (u_{\min}^2 + \tilde{d}), \end{aligned} \tag{40}$$

where C_1 is a positive constant. Because $\bar{e}_1^2 + \bar{x}_1^2$ is bounded on $[t_2, t_f)$ and $\lim_{x\to+\infty} l(t) = +\infty$, there exists a finite time t_3 ($t_2<t_3<t_f$) that makes the following inequality hold:

$$\dot{V}_1 \leq 2C_1 l V_1 + (u_{\min}^2 + \tilde{d}), \quad \forall t \in [t_3, t_f). \tag{41}$$

Thus, for any time $t_4 \in [t_3, t_f)$, it is suggested that

$$\dot{V}_1 \leq 2C_1 l(t_4) V_1 + (u_{\min}^2 + \tilde{d}), \quad \forall t \in [t_4, t_f). \tag{42}$$

Then we have

$$\begin{aligned} V_1(t) &\leq \mathrm{e}^{-C_1 l(t_4)(t-t_4)} V_1(t_4) \\ &\quad + \frac{u_{\min}^2 + \tilde{d}}{C_1 l(t_4)}\left[1 - \mathrm{e}^{-C_1 l(t_4)(t-t_4)}\right], \forall t \in [t_4, t_f). \end{aligned} \tag{43}$$

Furthermore,

$$\begin{aligned} V_1(t) &\leq \mathrm{e}^{-C_1 l(t_4)} V_1(t_4) + \frac{\tilde{d}}{C_1 l(t_4)} \\ &\leq \frac{2}{C_1^2 l^2(t_4)} V_1(t_4) + \frac{u_{\min}^2 + \tilde{d}}{C_1 l(t_4)}, \ \forall t \in [t_4 + 1, t_f). \end{aligned} \tag{44}$$

Because $\lambda_1\|\bar{\boldsymbol{e}}\|^2 \le \bar{\boldsymbol{e}}^{\mathrm{T}}\boldsymbol{P}_1\bar{\boldsymbol{e}}$ and $\lambda_2\|\bar{\boldsymbol{x}}\|^2 \le \bar{\boldsymbol{x}}^{\mathrm{T}}\boldsymbol{P}_2\bar{\boldsymbol{x}}$, we find that on $[t_4+1, t_f)$,

$$\begin{aligned} l^{2\mu}\bar{e}_1^2 + l^{2\mu}\bar{x}_1^2 &\le \left(\frac{1}{\eta\lambda_1}+\frac{1}{\lambda_2}\right)V_1 \\ &\le \left(\frac{1}{\eta\lambda_1}+\frac{1}{\lambda_2}\right)\left(\frac{2V_1(t_4)}{C_1^2 l^2(t_4)}+\frac{(u_{\min}^2+\tilde{d})}{C_1 l(t_4)}\right). \end{aligned} \tag{45}$$

This means that a sufficiently large t_4 exists, making $l^{2\mu}\bar{e}_1^2 + l^{2\mu}\bar{x}_1^2 \le \varsigma$ hold on $[t_4+1, t_f)$. Therefore, $\dot{l} = \max\left\{l^{2\mu}\bar{e}_1^2 + l^{2\mu}\bar{x}_1^2 - \varsigma, 0\right\} = 0$ on $[t_4+1, t_f)$. This is not consistent with the assumption $\lim_{x\to+\infty} l(t) = +\infty$.

Based on the above analysis, $l(t)$ can remain bounded with $t\in[0, t_f)$.

4.2 Boundedness proof of $\bar{\boldsymbol{x}}(t)$

For the state $\bar{\boldsymbol{x}}(t)$, we set the Lyapunov function as

$$V_{\bar{x}} = \bar{\boldsymbol{x}}^{\mathrm{T}}\boldsymbol{P}_2\bar{\boldsymbol{x}}. \tag{46}$$

According to Eq. (18) and inequalities (7), (11), and (30), we have

$$\begin{aligned} \dot{V}_{\bar{x}} &\le -3\sigma_1 l\|\bar{\boldsymbol{x}}\|^2 + 2l\bar{\boldsymbol{x}}^{\mathrm{T}}\boldsymbol{P}_2\boldsymbol{a}\bar{e}_1 + 2\bar{\boldsymbol{x}}^{\mathrm{T}}\boldsymbol{P}_2\boldsymbol{b}\frac{q(v)-v}{l^{n-1+\mu}} \\ &\quad -\frac{\dot{l}}{l}\bar{\boldsymbol{x}}^{\mathrm{T}}(\boldsymbol{D}\boldsymbol{P}_2+\boldsymbol{P}_2\boldsymbol{D}+2\mu\boldsymbol{P}_2)\bar{\boldsymbol{x}} \\ &\le -\frac{1}{2}\sigma_1 l\|\bar{\boldsymbol{x}}\|^2 + \frac{\|\boldsymbol{P}_2\boldsymbol{a}\|^2}{\sigma_1}l^{1-2\mu}(l+\varsigma) + u_{\min}^2 \\ &\le -C_2 V_{\bar{x}} + C_3(\dot{l}+\varsigma) + C_4, \end{aligned} \tag{47}$$

where $C_2 = \sigma_1/(2\|\boldsymbol{P}_2\|)$, $C_3 = \|\boldsymbol{P}_2\boldsymbol{a}\|^2 l^{1-2\mu}(t_f)/\sigma_1$, and $C_4 = u_{\min}^2$. It suggests that

$$\begin{aligned} V_{\bar{x}}(t) &\le \mathrm{e}^{-C_2 t}\int_0^t \mathrm{e}^{C_2\tau}\left[C_3(\dot{l}+\varsigma)+C_4\right]\mathrm{d}\tau + \mathrm{e}^{-C_2 t}V_{\bar{x}}(0) \\ &= \mathrm{e}^{-C_2 t}V_{\bar{x}}(0) + \frac{C_3\varsigma+C_4}{C_2}(1-\mathrm{e}^{-C_2 t}) \\ &\quad + C_3\mathrm{e}^{-C_2 t}\left(\mathrm{e}^{C_2 t}l(t) - 1 - C_2\int_0^t \mathrm{e}^{C_2\tau}l(\tau)\mathrm{d}\tau\right) \\ &\le V_{\bar{x}}(0) + C_3 l(t) + \frac{C_3\varsigma+C_4}{C_2}. \end{aligned} \tag{48}$$

With the boundedness of $l(t)$, we can find that $\bar{\boldsymbol{x}}(t)$ remains bounded with $t\in[0, t_f)$.

4.3 Boundedness proof of $\bar{\boldsymbol{e}}(t)$

State $\boldsymbol{e}$'s dynamics can be rewritten as

$$\begin{aligned} \dot{\boldsymbol{e}} &= (\boldsymbol{A} - ll^*\boldsymbol{L}_1\boldsymbol{L}_1^*\boldsymbol{a}\boldsymbol{c}^{\mathrm{T}})\boldsymbol{e} + ll^*\boldsymbol{L}_1\boldsymbol{L}_1^*\boldsymbol{a}e_1 \\ &\quad - l\boldsymbol{L}_1\boldsymbol{a}e_1 + \boldsymbol{\Phi} + \boldsymbol{d} - \dot{\boldsymbol{Y}}_{\mathrm{r}}, \end{aligned} \tag{49}$$

where $l^* \ge 32\eta n^4\|\boldsymbol{P}_1\|^2\theta^2/\sigma_1 + 1$,

$$\boldsymbol{L}_1^* = \begin{bmatrix} 1 & & & \\ & l^* & & \\ & & \ddots & \\ & & & (l^*)^{n-1} \end{bmatrix}, \boldsymbol{L}_1 = \begin{bmatrix} 1 & & & \\ & l & & \\ & & \ddots & \\ & & & l^{n-1} \end{bmatrix}. \tag{50}$$

Set $\boldsymbol{L}^* = (l^*)^{\mu}\boldsymbol{L}_1^*$. Based on the transformation $\boldsymbol{e}^* = (\boldsymbol{L}\boldsymbol{L}^*)^{-1}\boldsymbol{e}$ and Eq. (49), $\dot{\boldsymbol{e}}^*$ can be calculated.

Now a quadratic Lyapunov function is defined by

$$V_{e^*} = (\boldsymbol{e}^*)^{\mathrm{T}}\boldsymbol{P}_1\boldsymbol{e}^*. \tag{51}$$

Then the time derivative of V_{e^*} can be calculated as

$$\begin{aligned} \dot{V}_{e^*} &\le -\frac{1}{2}\sigma_1 ll^*\|\boldsymbol{e}^*\|^2 + 2ll^*(\boldsymbol{e}^*)^{\mathrm{T}}\boldsymbol{P}_1\boldsymbol{a}e_1^* \\ &\quad +2\|\boldsymbol{e}^*\|\|\boldsymbol{P}_1\|\left\|(\boldsymbol{d}+\boldsymbol{\Phi}-\dot{\boldsymbol{Y}}_{\mathrm{r}})(\boldsymbol{L}\boldsymbol{L}^*)^{-1}\right\| \\ &\quad -\frac{2}{\eta}\left(|y|^p+1\right)^2\|\boldsymbol{e}^*\|^2 - 2l(\boldsymbol{e}^*)^{\mathrm{T}}\boldsymbol{P}_1(\boldsymbol{L}_1^*)^{-1}\boldsymbol{a}e_1^*. \end{aligned} \tag{52}$$

According to $(e_1^*)^2 < \bar{e}_1^2$ and completion of the square, we have

$$\begin{aligned} 2ll^*(\boldsymbol{e}^*)^{\mathrm{T}}\boldsymbol{P}_1\boldsymbol{a}e_1^* &\le \frac{\sigma_1 ll^*}{8}\|\boldsymbol{e}^*\|^2 + \frac{8ll^*\|\boldsymbol{P}_1\boldsymbol{a}\|^2}{\sigma_1}(e_1^*)^2 \\ &\le \frac{\sigma_1 ll^*}{8}\|\boldsymbol{e}^*\|^2 + \frac{8ll^*\|\boldsymbol{P}_1\boldsymbol{a}\|^2}{\sigma_1}\bar{e}_1^2, \\ -2l(\boldsymbol{e}^*)^{\mathrm{T}}\boldsymbol{P}_1(\boldsymbol{L}_1^*)^{-1}\boldsymbol{a}e_1^* &\le \frac{\sigma_1 ll^*}{8}\|\boldsymbol{e}^*\|^2 + \frac{8l\|\boldsymbol{P}_1\|^2\|\boldsymbol{a}\|^2}{\sigma_1 l^*}(e_1^*)^2 \\ &\le \frac{\sigma_1 ll^*}{8}\|\boldsymbol{e}^*\|^2 + \frac{8l\|\boldsymbol{P}_1\|^2\|\boldsymbol{a}\|^2}{\sigma_1 l^*}\bar{e}_1^2. \end{aligned} \tag{53}$$

Similar to inequality (25), we have

$$\begin{aligned}&2\left\|\boldsymbol{e}^{*}\right\|\left\|\boldsymbol{P}_{1}\right\|\left\|(\boldsymbol{L}\boldsymbol{L}^{*})^{-1}(\boldsymbol{\Phi}+\boldsymbol{d}-\dot{\boldsymbol{Y}}_{\mathrm{r}})\right\|\\&\quad\le 2\eta n^{4}\left\|\boldsymbol{P}_{1}\right\|^{2}\theta^{2}\left\|\boldsymbol{e}^{*}\right\|^{2}+\frac{2}{\eta}\left(1+|y|^{p}\right)^{2}\left\|\boldsymbol{e}^{*}\right\|^{2}\\&\quad\quad+2\eta n^{4}\left\|\boldsymbol{P}_{1}\right\|^{2}\theta^{2}\left\|\bar{\boldsymbol{x}}\right\|^{2}+\frac{\sigma_{1}ll^{*}}{8}\left\|\boldsymbol{e}^{*}\right\|^{2}+\frac{2}{\eta}\tilde{d}.\end{aligned}\tag{54}$$

Substituting inequalities (53) and (54) into inequality (52), we have

$$\begin{aligned}\dot{V}_{e^{*}}\le&-\frac{1}{8}\sigma_{1}ll^{*}\left\|\boldsymbol{e}^{*}\right\|^{2}+2\eta n^{4}\left\|\boldsymbol{P}_{1}\right\|^{2}\theta^{2}\left\|\boldsymbol{e}^{*}\right\|^{2}\\&+\frac{8l^{1-2\mu}\left\|\boldsymbol{P}_{1}\right\|^{2}\left\|\boldsymbol{a}\right\|^{2}}{\sigma_{1}l^{*}}\bar{e}_{1}^{2}+2\eta n^{4}\left\|\boldsymbol{P}_{1}\right\|^{2}\theta^{2}\left\|\bar{\boldsymbol{x}}\right\|^{2}\\&+\frac{8ll^{*}\left\|\boldsymbol{P}_{1}\boldsymbol{a}\right\|^{2}}{\sigma_{1}}\bar{e}_{1}^{2}+\frac{2}{\eta}\tilde{d}.\end{aligned}\tag{55}$$

Because $l^{*}\ge 32\eta n^{4}\left\|\boldsymbol{P}_{1}\right\|^{2}\theta^{2}/\sigma_{1}+1$ and $l^{2\mu}\bar{e}_{1}^{2}\le \dot{l}+\varsigma$, we have

$$\begin{aligned}\dot{V}_{e^{*}}\le&-\frac{1}{16}\sigma_{1}ll^{*}\left\|\boldsymbol{e}^{*}\right\|^{2}+\frac{8l^{1-2\mu}l^{*}\left\|\boldsymbol{P}_{1}\boldsymbol{a}\right\|^{2}}{\sigma_{1}}(\dot{l}+\varsigma)\\&+\frac{8l^{1-2\mu}\left\|\boldsymbol{P}_{1}\right\|^{2}\left\|\boldsymbol{a}\right\|^{2}}{\sigma_{1}l^{*}}(\dot{l}+\varsigma)\\&+2\eta n^{4}\left\|\boldsymbol{P}_{1}\right\|^{2}\theta^{2}\left\|\bar{\boldsymbol{x}}\right\|^{2}+\frac{2}{\eta}\tilde{d}.\end{aligned}\tag{56}$$

Similar to inequalities (47) and (48), the boundedness of $\boldsymbol{e}^{*}$ can be proved by inequality (56). Furthermore, with $\boldsymbol{e}^{*}=(\boldsymbol{L}\boldsymbol{L}^{*})^{-1}\boldsymbol{e}=(\boldsymbol{L}^{*})^{-1}\bar{\boldsymbol{e}}$, we conclude that state $\bar{\boldsymbol{e}}$ remains bounded on $[0, t_{\mathrm{f}})$.

5 Simulation

Simulations were performed to validate the performance of the established method. The multi-agent system consisted of four agents that can be described by Eq. (1) and the mass M_i was set to be 1 kg. $q(u_{ix})$ and $q(u_{iy})$, the hysteretic quantizers, are described by Eq. (5) and $u_{\min}$=0.02. The reference trajectory was designed as a circle with p_{rx}=cos(0.3t) and p_{ry}=sin(0.3t). The system was a wedge-shaped formation that consisted of four agents. The starting positions of the four agents were chosen as (0.5, 0.5), (0.4, 0.4), (0.6, 0.2), and (0.6, 0.1).

For each agent, Assumption 2 holds for p=1. To satisfy the inequality $0<2\mu p<1$, the design parameter μ was chosen as 0.22. With the limitation of Lemma 2 and inequality (30), the relevant parameters were set as ς=0.15, $[a_{i1}, a_{i2}]^{\mathrm{T}}=[2.0, 1.0]^{\mathrm{T}}$, α_1=0.25, α_2=12.0, and $[k_{i1}, k_{i2}]^{\mathrm{T}}=[1.0, 2.0]^{\mathrm{T}}$.

In the simulation, we set the unknown parameter θ_i=10. The quantization parameter was given by δ=0.3. The trajectories of the four agents are shown in Fig. 2. Fig. 3 shows the dynamic gains l_{2x} and l_{2y} of the 2nd agent.

It can be seen that all the agents can track the reference trajectory and build the formation shape at the same time. Fig. 3 suggests that the dynamic gains are bounded.

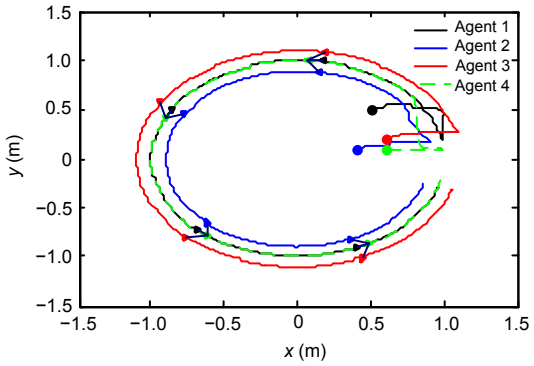

Fig. 2 Formation trajectory

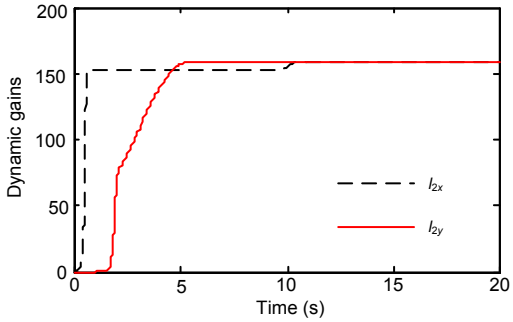

Fig. 3 Dynamic gain *l*

The tracking errors of all the agents in the direction of the x axis are shown in Fig. 4, and the agents' tracking errors in the direction of the y axis are shown in Fig. 5.

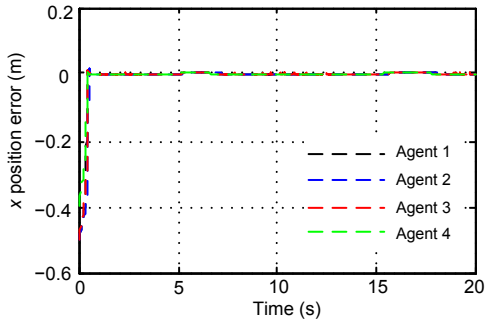

Fig. 4 Trajectory tracking errors x_e

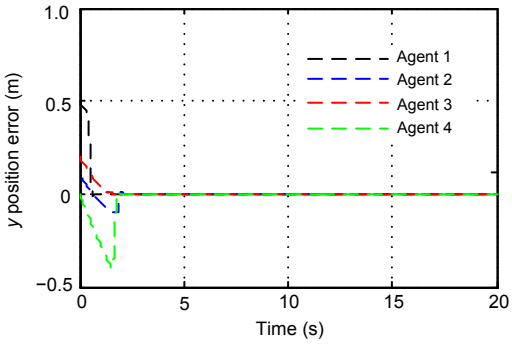

Fig. 5 Trajectory tracking errors y_e

We can figure out that the tracking errors converge to a small neighborhood of the origin asymptotically. It proves that unmanned aerial vehicle (UAV) formation can maintain the formation shape and track the reference trajectory.

Fig. 6 shows the quantized inputs of one typical agent, i.e., the 3rd agent. Fig. 7 shows an example of the analysis of the observer state.

From Fig. 6, we can see that the quantized inputs highly reduce the input signal. Fig. 7 suggests that the state estimates are bounded.

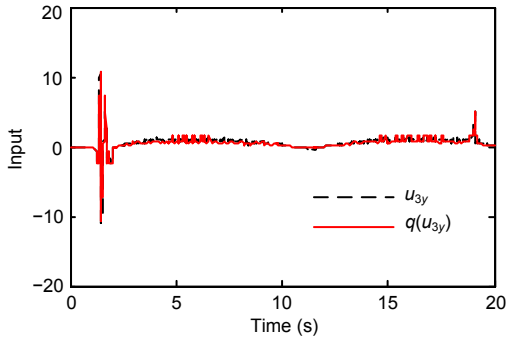

Fig. 6 The 3rd agent quantized input

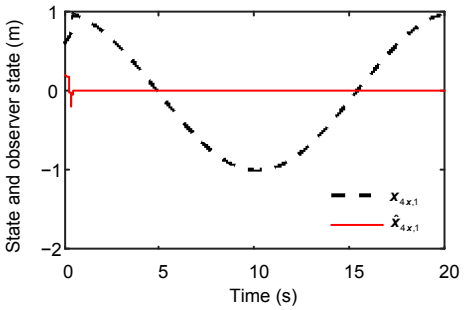

Fig. 7 State $x_{4x,1}$ and its estimate $\hat{x}_{4x,1}$

6 Conclusions

An adaptive output feedback controller has been presented for formation tracking of multiagent systems with uncertainties and quantized input signals based on a hysteretic quantizer and a high-gain dynamic observer. The system consists of multiple nonlinear agents that are established with immeasurable states and unknown parameters. It has been proved that all the system signals are bounded and that all the agents can maintain the prescribed formation shape while tracking the reference trajectory with tracking errors within a small neighborhood of the origin. The effectiveness of the system has been validated by simulations.

References

Bae J, Kim Y, 2012. Adaptive controller design for spacecraft formation flying using sliding mode controller and neural networks. *J Franklin Inst*, 349(2):578-603. https://doi.org/10.1016/j.jfranklin.2011.08.009

Briñón-Arranz L, Seuret A, Canudas-de-Wit C, 2014. Cooperative control design for time-varying formations of multi-agent systems. *IEEE Trans Autom Contr*, 59(8): 2283-2288. https://doi.org/10.1109/TAC.2014.2303213

Fu JJ, Wang JZ, 2014. Adaptive coordinated tracking of multi-agent systems with quantized information. *Syst Contr Lett*, 74:115-125. https://doi.org/10.1016/j.sysconle.2014.08.009

Hayakawa T, Ishii H, Tsumura K, 2009. Adaptive quantized control for nonlinear uncertain systems. *Syst Contr Lett*, 58(9):625-632. https://doi.org/10.1016/j.sysconle.2008.12.007

He L, Sun XX, Lin Y, 2017. Distributed adaptive control for time-varying formation tracking of a class of networked nonlinear systems. *Int J Contr*, 90(7):1319-1326. https://doi.org/10.1080/00207179.2016.1205757

He WL, Zhang B, Han QL, et al., 2017. Leader-following consensus of nonlinear multiagent systems with stochas-

tic sampling. *IEEE Trans Cybern*, 47(2):327-338. https://doi.org/10.1109/TCYB.2015.2514119

Jiang ZP, Liu TF, 2013. Quantized nonlinear control—a survey. *Acta Autom Sin*, 39(11):1820-1830. https://doi.org/10.3724/SP.J.1004.2013.01820

Li GQ, Lin Y, Zhang X, 2017. Adaptive output feedback control for a class of nonlinear uncertain systems with quantized input signal. *Int J Rob Nonl Contr*, 27(1):169-184. https://doi.org/10.1002/rnc.3569

Liu JL, Elia N, 2004. Quantized feedback stabilization of non-linear affine systems. *Int J Contr*, 77(3):239-249. https://doi.org/10.1080/00207170310001655336

Liu TF, Jiang ZP, Hill DJ, 2012. A sector bound approach to feedback control of nonlinear systems with state quantization. *Automatica*, 48(1):145-152. https://doi.org/10.1016/j.automatica.2011.09.041

Liu Y, Jia Y, 2012. Adaptive leader-following consensus control of multi-agent systems using model reference adaptive control approach. *IET Contr Theory Appl*, 6(13): 2002-2008. https://doi.org/10.1049/iet-cta.2011.0649

Liu YF, Zhao Y, Chen GR, 2016. Finite-time formation tracking control for multiple vehicles: a motion planning approach. *Int J Rob Nonl Contr*, 26(14):3130-3149. https://doi.org/10.1002/rnc.3496

Lu XQ, Wang YN, Mao JX, 2014. Nonlinear control for multiagent formations with delays in noisy environments. *Acta Autom Sin*, 40(12):2959-2967. https://doi.org/10.1016/S1874-1029(15)60001-5

Mahmood A, Kim Y, 2015. Leader-following formation control of quadcopters with heading synchronization. *Aerosp Sci Technol*, 47:68-74. https://doi.org/10.1016/j.ast.2015.09.009

Praly L, Jiang ZP, 2004. Linear output feedback with dynamic high gain for nonlinear systems. *Syst Contr Lett*, 53(2): 107-116. https://doi.org/10.1016/j.sysconle.2004.02.025

Rezaee H, Abdollahi F, 2014. A decentralized cooperative control scheme with obstacle avoidance for a team of mobile robots. *IEEE Trans Ind Electron*, 61(1):347-354. https://doi.org/10.1109/TIE.2013.2245612

Wan Y, Wen GH, Cao JD, et al., 2016. Distributed node-to-node consensus of multi-agent systems with stochastic sampling. *Int J Rob Nonl Contr*, 26(1):110-124. https://doi.org/10.1002/rnc.3302

Wan Y, Cao JD, Wen GH, 2017. Quantized synchronization of chaotic neural networks with scheduled output feedback control. *IEEE Trans Neur Netw Learn Syst*, 28(11):2638-2647. https://doi.org/10.1109/TNNLS.2016.2598730

Wen GH, Yu WW, Hu GQ, et al., 2015. Pinning synchronization of directed networks with switching topologies: a multiple Lyapunov functions approach. *IEEE Trans Neur Netw Learn Syst*, 26(12):3239-3250. https://doi.org/10.1109/TNNLS.2015.2443064

Zhao Y, Liu YF, Duan ZS, et al., 2016a. Distributed average computation for multiple time-varying signals with output measurements. *Int J Rob Nonl Contr*, 26(13):2899-2915. https://doi.org/10.1002/rnc.3486

Zhao Y, Duan ZS, Wen GH, et al., 2016b. Distributed finite-time tracking of multiple non-identical second-order nonlinear systems with settling time estimation. *Automatica*, 64:86-93. https://doi.org/10.1016/j.automatica.2015.11.005

Zhao Y, Liu YF, Li ZK, et al., 2017. Distributed average tracking for multiple signals generated by linear dynamical systems: an edge-based framework. *Automatica*, 75:158-166. https://doi.org/10.1016/j.automatica.2016.09.005

Zhou J, Wen CY, Yang GH, 2014. Adaptive backstepping stabilization of nonlinear uncertain systems with quantized input signal. *IEEE Trans Autom Contr*, 59(2):460-464. https://doi.org/10.1109/TAC.2013.2270870